EJN fens EUROPEAN JOURNAL OF NEUROSCIENCE

European Journal of Neuroscience, Vol. 38, pp. 3567–3579, 2013 doi:10.1111/ejn.12357

MOLECULAR AND SYNAPTIC MECHANISMS

Upregulation of axon guidance molecules in the adult central nervous system of Nogo-A knockout mice restricts neuronal growth and regeneration

Anissa Kempf,[1,*] Laura Montani,[1,†,*] Marija M. Petrinovic,[1,‡,*] Aileen Schroeter,[1,§] Oliver Weinmann,[1] Andrea Patrignani[2] and Martin E. Schwab[1]

[1]Department of Health Sciences and Technology, Brain Research Institute, University of Zurich, Swiss Federal Institute of Technology (ETH) Zurich, Winterthurerstrasse 190, CH-8057 Zurich, Switzerland

[2]Functional Genomics Center, University of Zurich, Winterthurerstrasse 190, CH-8057 Zurich, Switzerland

Keywords: compensation, EphA4, EphrinA3, myelin, Nogo-A, spinal cord injury

Abstract

Adult central nervous system axons show restricted growth and regeneration properties after injury. One of the underlying mechanisms is the activation of the Nogo-A/Nogo receptor (NgR1) signaling pathway. Nogo-A knockout (KO) mice show enhanced regenerative growth *in vivo*, even though it is less pronounced than after acute antibody-mediated neutralization of Nogo-A. Residual inhibition may involve a compensatory component. By mRNA expression profiling and immunoblots we show increased expression of several members of the Ephrin/Eph and Semaphorin/Plexin families of axon guidance molecules, e.g. EphrinA3 and EphA4, in the intact spinal cord of adult Nogo-A KO vs. wild-type (WT) mice. EphrinA3 inhibits neurite outgrowth of EphA4-positive neurons *in vitro*. In addition, EphrinA3 KO myelin extracts are less growth-inhibitory than WT but more than Nogo-A KO myelin extracts. EphA4 KO cortical neurons show decreased growth inhibition on Nogo-A KO myelin as compared with WT neurons, supporting increased EphA4-mediated growth inhibition in Nogo-A KO mice. Consistently, *in vivo*, Nogo-A/EphA4 double KO mice show increased axonal sprouting and regeneration after spinal cord injury as compared with EphA4 KO mice. Our results reveal the upregulation of developmental axon guidance cues following constitutive Nogo-A deletion, e.g. the EphrinA3/EphA4 ligand/receptor pair, and support their role in restricting neurite outgrowth in the absence of Nogo-A.

Introduction

Adult central nervous system (CNS) injuries result in chronic functional impairment as a consequence of the extremely limited ability of lesioned axons to successfully regrow and repair the damaged neuronal network (Yiu & He, 2006; Schwab, 2010). CNS regeneration is prevented by various cell-intrinsic suppressors of growth signaling, e.g. phosphatase and tensin homolog (PTEN; Park *et al.*, 2008), as well as by cell-extrinsic mechanisms (Yiu & He, 2006). The latter include growth inhibitory factors present in the glial scar, e.g. chondroitin sulfate proteoglycans (Bradbury *et al.*, 2002; Fawcett, 2006), as well as in myelin, e.g. Nogo-A (Chen *et al.*, 2000; GrandPre *et al.*, 2000; Prinjha *et al.*, 2000), myelin-associated glycoprotein (MAG; McKerracher *et al.*, 1994; Mukhopadhyay *et al.*, 1994), oligodendrocyte myelin glycoprotein (OMgp; Wang *et al.*, 2002) or the lipid sulfatide (Winzeler *et al.*, 2011). In the last decade, several scar- or myelin-associated developmental axon guidance molecules and their receptors have been shown to possess growth-inhibitory properties – repulsive guidance molecule RGMa (Hata *et al.*, 2006), EphrinB3 (Benson *et al.*, 2005; Duffy *et al.*, 2012), EphA4 (Goldshmit *et al.*, 2004, 2011; Fabes *et al.*, 2006), EphB3 (Liu *et al.*, 2006), Sema3A (Kaneko *et al.*, 2006; Pasterkamp & Verhaagen, 2006; Montolio *et al.*, 2009), Sema4D (Moreau-Fauvarque *et al.*, 2003), Sema5A (Goldberg *et al.*, 2004), Netrin1 (Low *et al.*, 2008) and PlexinA2 (Shim *et al.*, 2012).

Among myelin-associated growth inhibitors, Nogo-A has been most extensively studied *in vitro* and *in vivo*. Neutralization via function-blocking antibodies led to regenerative growth and enhanced sprouting and plasticity in rodent and primate models of spinal cord injury (Zorner & Schwab, 2010), paving the way for clinical trials in acute spinal cord-injured, amyotrophic lateral sclerosis and multiple sclerosis patients (ClinicalTrials.gov – NCT00406016, NCT00875446 and NCT01424423; Buchli *et al.*, 2007). Similar results were obtained by blocking the Nogo-A receptor NgR1 (Akbik *et al.*, 2012). Despite the consistent association of acute Nogo-A or NgR1 blockade with

Correspondence: Dr A. Kempf, as above.
E-mail: kempf@hifo.uzh.ch.

*These authors contributed equally to this study.

†*Present address*: Institute of Molecular Health Sciences, Swiss Federal Institute of Technology, ETH, Schafmattstrasse 22, CH-8093 Zurich, Switzerland

‡*Present address*: F. Hoffmann-La Roche AG, Pharma Research and Early Development, pRED, DTA Neuroscience, Grenzacherstrasse 124, CH-4070 Basel, Switzerland

§*Present address*: Institute for Biomedical Engineering, Swiss Federal Institute of Technology, ETH, Zurich, Schafmattstrasse 22, CH-8093 Zurich, Switzerland

Received 26 June 2013, revised 14 August 2013, accepted 15 August 2013

increased axonal sprouting and regeneration after CNS injury, the generation of different Nogo-A, Nogo-A/B or Nogo-A/B/C knockout (KO) mice by several laboratories led to more moderate and controversial phenotypes (Kim *et al.*, 2003; Simonen *et al.*, 2003; Zheng *et al.*, 2003; Dimou *et al.*, 2006; Lee *et al.*, 2009, 2010; Cafferty *et al.*, 2010). These were attributed to differences in Nogo deletion mutants, mouse strain genetic background effects, differences in experimental protocols, or possible compensation by other Nogo isoforms, other reticulon proteins or functionally related genes (Schwab, 2004; Lee & Zheng, 2012; Tews *et al.*, 2013). However, genetic compensation in Nogo-A KO mice as well as its functional implication with regard to axonal growth and regeneration has not yet been systematically addressed.

By performing a microarray screen, we investigated the upregulation of potential subsidiary inhibitors in the spinal cord of adult Nogo-A KO mice. We found an upregulation of several axon guidance molecules, and identified EphrinA3 as a novel neuronal growth inhibitor signaling via the receptor EphA4. Our results suggest a role for EphA4 in partially mediating the residual inhibition observed in Nogo-A KO mice.

Material and methods

Experimental animals

All animal experiments were performed with the approval and in accordance with the guidelines of the Zurich Cantonal Veterinary Office. Experiments were carried out in accordance with the European Communities Council Directive of 24 November 1986 (86/609/EEC). All efforts were made to minimize the number of animals required. Postnatal day 5–8 (P5–8) and adult C57BL/6 male and female wild-type (WT), Nogo-A KO (Simonen *et al.*, 2003; Dimou *et al.*, 2006), EphA4 KO (Dottori *et al.*, 1998; Kullander *et al.*, 2001) and Nogo-A/EphA4 double KO mice were used in this study. All lines were backcrossed for at least ten generations and maintained on a pure C57BL/6 background to exclude strain-specific effects. EphA4 KO mice (Dottori *et al.*, 1998; Kullander *et al.*, 2001) were kindly provided by R. Klein (Max-Planck Institute for Neurobiology, Martinsried, Germany). Nogo-A/EphA4 double KO mice were generated by crossing Nogo-A KO with EphA4 KO mice. EphrinA3 KO (Cutforth *et al.*, 2003) spinal cord tissue was a generous gift from D. Feldheim (University of California, Santa Cruz, CA, USA).

Antibodies and recombinant proteins

The following antibodies were used (including dilutions used for Western blot (WB) and immunohistochemistry (IHC)) – mouse anti-EphA4 (WB 1 : 200; Cat. No. 37-1600; Invitrogen, Carlsbad, CA, USA; antibody specifically recognizes the C terminus of human EphA4 and cross-reacts with mouse), rabbit anti-EphrinA3 (WB 1 : 200, IHC 1 : 150; Cat. No. 36-7500; Invitrogen; antibody specifically recognizes the C terminus of mouse EphrinA3), rabbit anti-glial fibrillary acidic protein (GFAP; IHC 1 : 500; Cat. No. Z0334; DakoCytomation, Glostrup, Denmark; antibody specifically recognizes cow GFAP and cross-reacts with all mammalian GFAP), mouse anti-glyceraldehyde-3-phosphate dehydrogenase (GAPDH; WB 1 : 20,000; Cat. No. ab8245; Abcam, Cambridge, UK; antibody specifically recognizes rabbit GAPDH and cross-reacts with all mammalian GAPDH), rabbit anti-S/L myelin-associated glycoprotein (MAG; WB 1 : 1000; Cat. No. 34-6200; Invitrogen; antibody specifically recognizes human MAG and cross-reacts with rat MAG), rabbit anti-Nogo-A/B serum (Bianca, Rb1; Oertle *et al.* (2003); WB 1 : 15,000; antibody specifically recognizes the N terminus of rat Nogo-A/B (amino acids 1–31 + 59–172) and cross-reacts with mouse Nogo-A/B), mouse anti-NeuN (IHC 1 : 200; Cat. No. MAB377; Millipore, Billerica, MA, USA; antibody specifically recognizes mouse NeuN and cross-reacts with all mammalian NeuN), rabbit anti-Sema3F (WB 1 : 1000; Cat. No. ab135880; Abcam; antibody specifically recognizes the C terminus of human Sema3F and cross-reacts with mouse and rat Sema3F), mouse anti-Sema4D (WB 1 : 2000; Cat. No. 610670; BD Biosciences, Franklin Lakes, NJ, USA; antibody specifically recognizes human Sema4D (amino acids 721–861) and cross-reacts with rat and mouse), mouse anti-βIII Tubulin (ICC 1 : 2000; Cat. No. G7121; Promega, Madison, WI, USA; antibody specifically recognizes the C terminus of rat βIII Tubulin and cross-reacts with mouse), mouse anti-receptor interacting protein (RIP; Oligo; IHC 1 : 100; Cat. No. MAB1580; Millipore), goat anti-mouse IgG horseradish peroxidase (HRP)-conjugated (WB 1 : 15 000; Cat. No. 31446; Thermo Fisher Scientific, Waltham, MA, USA), donkey anti-rabbit IgG HRP-conjugated (WB 1 : 10 000; Cat. No. 31458; Thermo Fisher Scientific), goat anti-mouse IgG Cy3-conjugated (IHC 1 : 1000; Cat. No. 115-165-166; Jackson ImmunoResearch Laboratories, West Grove, PA, USA), goat anti-rabbit IgG Cy3-conjugated (IHC 1 : 1000; Cat. No. 115-165-003; Jackson ImmunoResearch Laboratories) and goat anti-rabbit IgG Alexa488-conjugated (IHC 1 : 1000; Cat. No. A11034; Invitrogen). EphrinA3 and EphA4 antibodies were validated with KO lysates.

The following recombinant proteins were used – human EphrinA3-Fc (Cat. No. 359EA; R&D Systems, Minneapolis, MN, USA), human Fc (Cat. No. 009-000-008; Jackson Laboratories) and goat anti-human IgG-Fcγ fragment (Cat. No. 109-005-098; Jackson Laboratories).

Affymetrix GeneChips

Lumbar spinal cords from three adult (3–4 months old) male WT and Nogo-A KO mice were dissected and transferred into 'RNA later' stabilization solution (Ambion, Austin, TX, USA). Total RNA extraction, cRNA preparation, array hybridization on GeneChip® Mouse Genome 430 2.0 arrays, data acquisition and analysis were performed as described previously (Craveiro *et al.*, 2008). Data were analysed applying a one-way analysis of variance (ANOVA; $P < 0.05$). A final threshold of ≥ 1.2-fold increase or decrease in the expression level of each single transcript was applied. Regulated transcripts were assigned to functional categories according to GeneOntology (http://www.geneontology.org) as well as literature and database mining (PubMed: http://www.pubmed.com; Bioinformatics Harvester EMBL Heidelberg: http://harvester.kit.edu/HarvesterPortal). GeneChip data are available online at the GEO database (http://www.ncbi.nlm.nih.gov/geo/query/acc.cgi?token=jlcnjkwuyccocxk&acc=GSE11276).

Quantitative real-time PCR (qRT-PCR)

Primer and probe sets were designed through Primer Express Software version 2.0 (Applied Biosystems, Carlsbad, CA, USA). Total RNA from three Nogo-A KO and three WT adult (4 months old) lumbar spinal cords was transcribed to cDNA using the TaqMan Reverse Transcription Reagents (Applied Biosystems) and TaqMan qRT-PCR was performed. Target amplification with TaqMan Universal PCR Master Mix for three replicates per sample was performed according to the manufacturer's instructions. Signal was detected with the ABI Prism 7700 Sequence Detection System (software version 1.6). Relative quantification was performed using the comparative CT method (Muller *et al.*, 2002). The 18S ribosomal subunit was used as an endogenous reference control. The following primers were

used: *EphrinA3* (Fwd 5′-TGTCTGAGGATGAAGGTGTTCG-3′, Rev 5′-GACCGGCTTCTCCCCG-3′); *EphA4* (Fwd 5′-GGCTCCTT GGATGCTTTCC-3′, Rev 5′-GCATGCCCACCAGCTGA-3′); *Semaphorin3F* (*Sema3F*, Fwd 5′-CATCAACCGAGAGCCCCTTA-3′, Rev 5′-ATGCACTCCTCAATGCGCT-3′); *Semaphorin4D* (*Sema4D*, Fwd 5′-CCTTGAGGACGGAGTATGCC-3′, Rev 5′-TCTGGATCA CGTCAGCAAAGA-3′); *PlexinB2* (Fwd 5′-CTTCCACGGAGAAAT CCAGT-3′, Rev 5′-GAGCCGCATGGGAAGC-3′); and *18S RNA* (Fwd 5′-CTTTGGTCGCTCGCTCCTC-3′, Rev 5′-CTGACCGGGTT GGTTTTGAT-3′).

To determine changes in EphrinA3 and GFAP expression 7 days after spinal cord injury (see below), a dissected spinal cord segment spanning the lesion site (5 mm) was dissected from four WT mice. Sham-operated mice were used as control ($n = 4$). Total RNA and cDNA was processed as described above. cDNA was amplified using the Light Cycler 480 thermocycler (Roche Diagnostics AG, Rotkreuz, Switzerland) with the polymerase ready mix (SYBR Green I Master; Roche Diagnostics AG). Relative quantification was performed using the comparative CT method. cDNA levels were normalized to the reference gene *Gapdh* (Fwd 5′-CAGCAATGCATCCTGCACC-3′, Rev 5′-TGGACTGTGGTCATGAGCCC-3′). The following primers were used for *GFAP* (Fwd 5′-CCAC CAAACTGGCTGATGTCTAC-3′, Rev 5′- TTCTCTCCAAATCCA CACGAGC -3′). Each reaction was done in triplicate.

Immunoblotting

Tissues were homogenized and proteins extracted on ice in lysis buffer (50 mM NaH_2PO_4 pH 8.0, 150 mM NaCl, 0.5% 3-[(3-cholamidopropyl)dimethylammonio]-1-propanesulfonate (CHAPS), protease inhibitors cocktail (Roche, Basel, Switzerland)) and processed as previously described (Montani *et al.*, 2009). Twenty or 40 μg protein was loaded per lane. Densitometry analysis was performed with IMAGEJ software (NIH, Bethesda, MD, USA). Values were normalized to the housekeeping gene GAPDH and to the mean value of the corresponding control group.

Cell culture

Dissociated cortical neurons

Cortices from P5–P8 mice were rapidly dissected in ice-cold Hibernate A medium (BrainBits, Springfield, IL, USA) supplemented with 1% penicillin/streptomycin (Gibco, Carlsbad, CA, USA), 2% B27 supplement (Gibco) and 200 mM L-glutamine (Gibco), and digested for 35 min at 30 °C with 2 mg/mL papain (Worthington, Lakewood, NJ, USA). After gentle trituration with a flame-polished Pasteur pipette, cortical neurons were purified from oligodendrocytes and microglial cells on an OptiPrep (Greiner, Monroe, NC, USA) density gradient. Cells were plated at 15 000 cells/cm^2 on glass coverslips coated with 1 μg/mL poly-L-ornithine (poly(O); Sigma, St Louis, MO, USA). Cultures were grown for 48 h at 37 °C/5% CO_2 in Neurobasal A medium (Gibco) supplemented with 1% penicillin/streptomycin (Gibco), 2% B27 (Gibco) and 200 mM L-glutamine (Gibco).

Dissociated dorsal root ganglia (DRG) neurons

DRG were removed from P5–P8 mice and processed as previously described (Montani *et al.*, 2009). DRG neurons were cultured at a density of 4500 cells/cm^2 for 10 h at 37 °C/5% CO_2 on glass coverslips coated with 20 μg/mL poly-L-lysine (PLL; Sigma) and 5 μg/mL laminin (Invitrogen).

Neurite outgrowth assays

For assays involving recombinant Fc chimeric proteins, EphrinA3-Fc was clustered with goat anti-human IgG-Fcγ in a ratio of 1 : 10 for 2 h at 37 °C. Glass coverslips were coated with poly(O) or PLL/laminin (see above) and overlaid with 50 nM clustered EphrinA3-Fc or control Fc in phosphate-buffered saline (PBS; 0.1 M, pH 7.4) for 2 h at 37 °C before plating of the cells. For outgrowth assays on myelin-enriched spinal cord lysates, membrane-enriched spinal cord extracts were prepared. Dissected spinal cords were homogenized and proteins extracted on ice in lysis buffer (20 mM Tris-HCl, pH 8.0, 60 mM CHAPS, 1 mM EDTA, 1 mM phenylmethanesulfonyl fluoride (PMSF), protease inhibitor cocktail (Complete Mini; Roche)). Lysates were enriched in membrane proteins by centrifugation for 1 h at 100 000 ***g*** at 4 °C in a Beckman TL-100 ultracentrifuge. Glass coverslips were coated with poly(O) and 6 μg/cm^2 spinal cord extracts for 2 h at 37 °C before plating of the cells.

Cells were fixed with 4% paraformaldehyde (PFA) and stained for βIII-Tubulin as previously described (Joset *et al.*, 2010). Cultures were imaged with a DFC 350 FX Leica camera in a Leica DM 5500 B microscope equipped with a 10 × objective (HCX PL FLUOTAR, NA 0.3). Neurite outgrowth was quantified using MetaMorph software (Visitron systems GmbH, Puchheim, Germany).

Spinal cord injury and corticospinal tract (CST) tracing

Twenty-week-old C57BL/6 WT ($n = 11$), Nogo-A KO ($n = 12$), EphA4 KO ($n = 13$) and Nogo-A/EphA4 double KO ($n = 11$) mice of either sex were deeply anaesthetized by intraperitoneal injection of Hypnorm (0.3 mg/kg body weight; Jansen Pharmaceuticals, Titusville, NJ, USA)/Dormicum (0.6 mg/kg body weight; Roche). A laminectomy was performed at thoracic level 8 (T8). The dura was opened and a bilateral lesion of the dorsal and the dorsolateral funiculi and the dorsal horns was produced with iridectomy scissors under a surgical microscope. Subsequently, back muscles were sutured and the skin was closed with surgical staples. For anterograde tracing of the CST, mice received four injections (0.5 μL each) of a 10% biotin dextran amine (BDA; 10 000 mol. wt; Invitrogen) solution in 0.1 M phosphate buffer (PB; pH 7.2) into the right sensory-motor cortex immediately after spinal cord injury. Animals were killed 24 days post-injury. To determine changes in EphrinA3 expression after spinal cord injury, four WT mice underwent a dorsal hemisection surgery. Four sham-operated WT mice were used as control. Tissue was dissected 7 days post-injury and processed as described above.

Immunohistochemistry

Tissue preparation

Animals were deeply anaesthetized with pentobarbital (Nembutal, 75 mg/100 g body weight; Abbott Laboratories, Abbott Park, IL, USA) and transcardially perfused with PBS followed by 4% PFA containing 5% sucrose. Spinal cords were dissected and postfixed in the same fixative overnight at 4 °C before they were cryoprotected in 30% sucrose, embedded in Tissue-Tek OCT compound (Sakura Finetechnical, Tokyo, Japan) and rapidly frozen in isopentane at −40 °C.

Immunofluorescence staining

Forty μm-thick cross or longitudinal sections were cut on a cryostat and transferred to ice-cold PBS for free-floating immunostaining.

Free aldehyde groups were quenched in antigen retrieval solution (0.1 M Tris, pH 8.0, 50 mM glycine) for 3 min at 80 °C. After permeabilization with 0.3% Triton X-100 for 20 min, sections were blocked with 4% goat serum in 0.1 M PB for 1 h. Primary antibodies were applied overnight at 4 °C. After washing, sections were incubated with the appropriate secondary antibodies for 2 h at room temperature. Sections were then counterstained with Hoechst dye 33342 (Invitrogen), mounted on Superfrost-Plus slides (Menzel-Gläser, Braunschweig, Germany) and coverslipped with Mowiol/2% DABCO (Sigma). Images were acquired with a cooled CCD camera (CoolSNAP HQ, Photometrics) on a Zeiss Axiophot microscope and collected using image analysis software MCID ELITE Software version 7.0 (Imaging Research). A 5 × objective (Plan NEOFLUAR, NA 0.15) was used. Single-cell densitometry analysis was performed using the IMAGEJ software (NIH; Version 1.44). The same exposure time was used for all images of a given staining. Ten images were taken from a region of interest and averaged for each animal. Mean gray level values were background-corrected and normalized to the mean value of the corresponding control group. Confocal images were acquired by using a TCS SP2 AOBS spectral confocal microscope (Leica Microsystems) with a 20 × (HC PL FLUOTAR, NA 0.50) or 63 × oil immersion objective (HCX PL APO Oil, NA 1.32).

Peroxidase diaminobenzidine staining

Thirty μm-thick sagittal sections comprising the lesion site and ~15 mm of the spinal cord caudal to the lesion site were cut on a cryostat. The medulla oblongata was cut in the transverse plane to control for labeling efficiency. Sections were stained for BDA according to the nickel-enhanced diaminobenzidine (DAB) protocol as described previously (Herzog and Brosamle, 1997). Subsequently, sections were dehydrated and coverslipped with Eukitt (Kindler, Freiburg im Breisgau, Germany).

Quantification of regenerative properties of the CST

Animals showing a smaller or bigger (almost complete transection) lesion of the CST were excluded from the study (WT: $n = 1$, EphA4 KO: $n = 2$, Nogo-A/EphA4 KO: $n = 2$). The number of CST sprouting fibers 1 mm rostral to the lesion site was assessed using a 0–3 point scoring scale (0, no sprouting; 1, single and short fine fibers; 2, longer fibers, rarely reaching the lesion center and rarely having growth cones; 3, dense outgrowth of fibers from the main CST toward and around the lesion, frequent growth cones) as previously described (Liebscher *et al.*, 2005; Dimou *et al.*, 2006). The number of labeled axons caudal to the lesion site was quantified on all adjacent sagittal sections of the traced half of the spinal cord using dorsoventral lines positioned at the lesion center and at 1, 3, 5 and 10 mm caudal to the lesion as described previously (Liebscher *et al.*, 2005; Dimou *et al.*, 2006). BDA tracing efficiency, expressed as the average number of BDA-positive CST axons in the medullary pyramids, was comparable between the genotypes (WT: 2126.38 ± 72.00, Nogo-A KO: 1958.06 ± 52.75, EphA4 KO: 1995.33 ± 47.22, Nogo-A/EphA4 KO: 2013.19 ± 78.16; $F_{3,38} = 2.542$, $P > 0.05$; one-way ANOVA). Thus, the obtained sum of fibers at each distance quantified was expressed as the raw number of axons per section.

Quantification of the lesion and scar volume

To visualize the lesion and the scar volume, all sagittal sections of each animal were immunostained with an anti-GFAP antibody. Lesion area was defined as the GFAP-negative area of the lesion core, whereas the scar area was defined as the GFAP-positive region surrounding the lesion core. Sections were reconstructed using a Neurolucida software-controlled computer system (MBF Bioscience, Williston, VT, USA) to estimate the lesion and scar volume. Images were taken under a Leica DM 5500 B microscope equipped with a 10 × objective (HCX PL FLUOTAR, NA 0.3).

Statistical analysis

Statistical analyses were conducted using the statistical software SPSS (IBM) and GRAPHPAD PRISM (GraphPad Software Inc., La Jolla, CA, USA). For quantification of neurite outgrowth, the mean ± SEM of neurite length for each condition (150–200 cells) was determined from multiple independent experiments. For quantification of immunoblots, the mean ± SEM of normalized densitometry values for each condition was determined from 3–4 mice. For quantification of immunohistochemistry, the mean ± SEM of normalized densitometry values for each condition (ten cells) was determined from three mice. Immunoblotting, immunohistochemical, neurite outgrowth and qRT-PCR data were analysed using an unpaired Student's t test (two-tailed). For quantification of regenerative growth, the number of BDA-positive axons at specified distances was counted as described above. The mean ± SEM of CST axons per section was determined from 9–12 mice and subjected to a Welch's t test to account for unequal variances and non-normal distributions. The mean ± SEM of sprouting fibers 1 mm rostral to the lesion site was determined from 9–12 mice and was analysed by a Welch's t test. The mean ± SEM of the lesion and scar volume was determined from 5–10 mice and subjected to a one-way ANOVA followed by a *post hoc* Bonferroni's test; n identifies the number of independent experiments or mice. A P value of less than 0.05 was considered statistically significant. All data are shown as mean values ± SEM with $*P < 0.05$, $**P < 0.01$ and $***P < 0.001$.

Results

Upregulation of developmental axon guidance molecules in the spinal cord of adult Nogo-A KO mice

To investigate compensatory changes due to the constitutive genetic ablation of Nogo-A, we compared the transcriptome of the intact lumbar spinal cord of adult C57BL/6 Nogo-A KO vs. WT mice. The Affymetrix GeneChip analysis revealed the statistically significant regulation of 606 transcripts above or below a 1.2-fold change threshold ($P < 0.05$; ANOVA). In total, 554 (91.4%) genes showed an increased expression, and 52 (8.6%) a decreased expression. The main represented functional categories, with assignments based on GeneOntology and literature mining, were – signaling (14%), transcription and RNA processing (13%), transport (9%), cell growth (9%), metabolism (7%), protein processing (6.5%), synapse related and vesicles (5.5%), axon guidance and cell adhesion (5%), DNA and chromatin processing (4.5%), proteolysis and peptidolysis (4%), defense/immune response (4%), cytoskeleton (3%), apoptosis (3%) and response to stress (1%; Fig. 1A, Supporting Information Table S1). In accordance with our previously published data showing a role for neuronal Nogo-A in remodeling of the growth cone cytoskeleton in the intact CNS (Montani *et al.*, 2009), we observed the upregulation of microtubule-associated proteins (TAU (1.54-fold), MAP1 (1.51-fold), moesin (1.30-fold)), actin-binding factors (gelsolin (1.62-fold), coronin (1.43-fold), talin (1.38-fold)), motor molecules (kinesin2

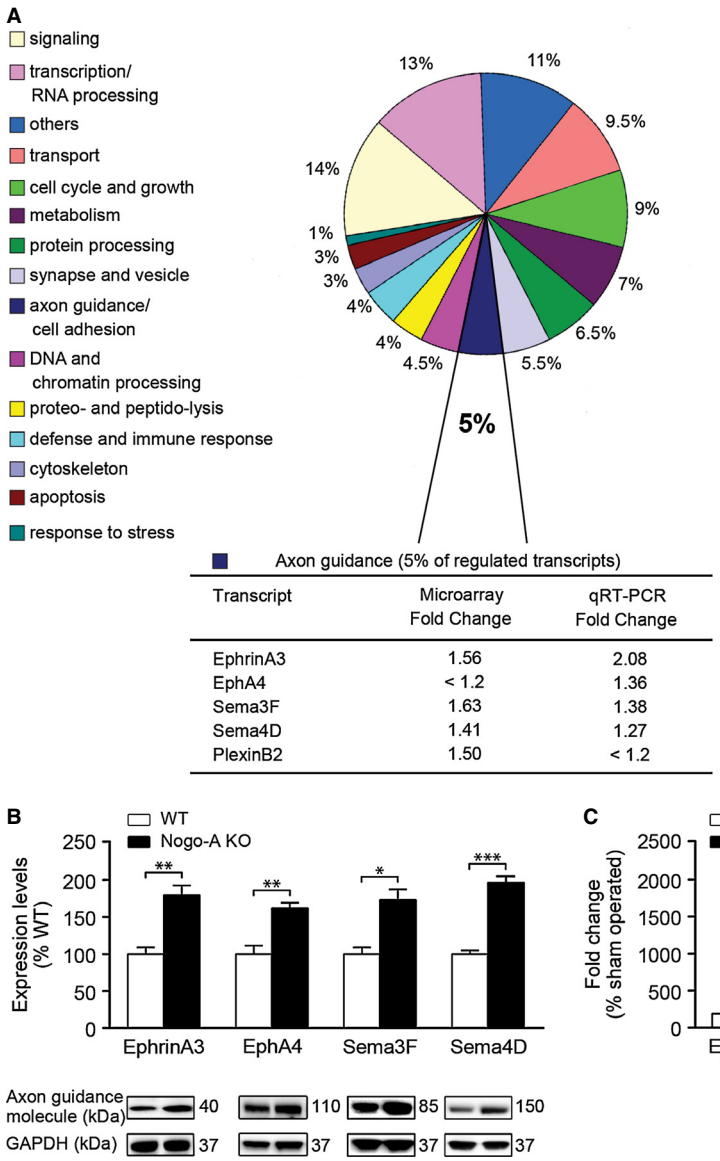

Transcript	Microarray Fold Change	qRT-PCR Fold Change
EphrinA3	1.56	2.08
EphA4	< 1.2	1.36
Sema3F	1.63	1.38
Sema4D	1.41	1.27
PlexinB2	1.50	< 1.2

FIG. 1. Transcriptomic profiling of the spinal cord of adult Nogo-A KO mice. (A) Percentage of total transcripts (n = 606) significantly regulated in the spinal cord of adult Nogo-A KO vs. WT mice and assigned to functional categories based on GeneOntology and literature and database mining. The further discussed category 'Axon guidance and cell adhesion' is highlighted. Expression changes of candidate axon guidance molecules regulated in the spinal cord of adult Nogo-A KO vs. WT mice (WT = 1) as assessed by microarray and qRT-PCR. A final threshold of a 1.2-fold increase or decrease in the expression level was applied. 18S RNA was used as housekeeping gene. (B) Western blot analyses of EphrinA3, EphA4, Sema3F and Sema4D expression in adult Nogo-A KO vs. WT spinal cord lysates and densitometry quantification thereof. Protein levels are normalized to GAPDH used as loading control. (C) qRT-PCR analysis of EphrinA3 and GFAP expression levels in sham-operated vs. lesioned WT spinal cord tissue 7 days post-injury. GAPDH was used as housekeeping gene. Data shown are means ± SEM (n = 3–4 mice; $^*P < 0.05$, $^{**}P < 0.01$, $^{***}P < 0.001$; Student's t test). DHx = dorsal hemisection.

(1.39-fold)) and cytoskeletal regulators (PAK4 (1.20-fold), RhoGDI (1.51-fold)) (Table S1).

To address a possible upregulation of growth-inhibitory molecules in Nogo-A KO mice, we focused on changes in the expression of the known myelin-associated growth inhibitors as well as on developmental repulsive/inhibitory axon guidance molecules. Analysis of the growth-inhibitory myelin proteins MAG and OMgp revealed a 1.46-fold upregulation of MAG mRNA, whereas no change was observed for OMgp (Table S1). Interestingly, specific members of the Sema/Plexin and Ephrin/Eph families of axon guidance molecules responded to the ablation of Nogo-A: the mRNA levels of Sema4D, Sema3F and the Sema receptor PlexinB2 were significantly upregulated by 1.31-, 1.63- and 1.50-fold, respectively (Fig. 1A). Among Ephrin/Eph members, EphrinA3 mRNA was found to be 1.56-fold enriched, whereas the change for EphA4 was below 1.2-fold (1.18) albeit significant (Fig. 1A). All observed transcriptional changes in Ephrin/Eph and Sema/Plexin family members were further verified by qRT-PCR. We confirmed significant changes for EphrinA3, Sema3F and Sema4D, and additionally showed a significant 1.36-fold upregulation of EphA4 (Fig. 1A), whose role in inhibiting CNS regeneration has been the object of recent studies (Goldshmit *et al.*, 2004, 2011; Cruz-Orengo *et al.*, 2006, 2007; Fabes *et al.*, 2006, 2007; Herrmann *et al.*, 2010b; Munro *et al.*, 2012).

EphrinA3 is upregulated in spinal cord oligodendrocytes and neurons of adult Nogo-A KO mice

We hypothesized that MAG as well as the guidance cues EphrinA3, EphA4, Sema3F and Sema4D might compensate for the lack of Nogo-A in Nogo-A KO mice. Their upregulation was therefore further investigated at the protein level by immunoblotting (Fig. 1B). MAG protein levels did not change significantly in Nogo-A KO spinal cord lysates (WT: 100.0 ± 4.5%, KO: 114.6 ± 7.6%; $P = 0.150$, $n = 4$; unpaired two-tailed Student's t test). However, we found that EphrinA3 ($t_6 = 4.948$, $P = 0.003$, $n = 4$), EphA4 ($t_6 = 4.613$, $P = 0.004$, $n = 4$), Sema3F ($t_4 = 4.305$, $P = 0.013$, $n = 3$) and Sema4D ($t_6 = 8.180$, $P < 0.0001$, $n = 4$) were significantly upregulated in Nogo-A KO spinal cord lysates (unpaired two-tailed Student's t test; Fig. 1B). The large fold change in EphrinA3 mRNA and protein (WT: 100.0 ± 9.1%, KO: 179.5 ± 13.3%, $n = 4$) expression as well as its unknown role for growth inhibition in the adult CNS prompted us to select EphrinA3 for further analysis. EphrinA3 can bind to several Ephrin receptors. Interestingly, a number of signaling components known to be modulated by the EphrinA3/EphA4 axis were also increased in the Nogo-A KO spinal cord, e.g. the Cyclin-dependent kinase 5 (Cdk5) regulators p35-Cdk5, Cables1 and Fnbp2/Cdkrap2 (Table S1). Together, these data point to a potential upregulation of EphrinA3/EphA4 signaling following constitutive genetic deletion of Nogo-A *in vivo*.

Sema4D, Sema3F and EphA4 have been reported to be upregulated following spinal cord injury and thereby to increase growth inhibition (Moreau-Fauvarque *et al.*, 2003; Goldshmit *et al.*, 2004; Lindholm *et al.*, 2004; Fabes *et al.*, 2006). To investigate changes in EphrinA3 expression 7 days post-injury, a semi-quantitative RT-PCR analysis of EphrinA3 in lesioned spinal cord tissue including the lesion site was performed. As opposed to GFAP ($t_6 = 6.399$, $P < 0.001$, $n = 4$), denoting reactive astrogliosis following injury (Fawcett, 2006), EphrinA3 mRNA levels did not significantly change when compared with sham-operated WT mice (Fig. 1C).

The cell type-specific localization of EphrinA3 in the adult spinal cord has not yet been addressed. Immunohistochemical analysis of EphrinA3 in the spinal cord of adult WT and Nogo-A KO mice revealed its expression in NeuN-positive neurons (Fig. 2A–C) but not in GFAP-positive astrocytes (Fig. 2D–F). Double immunostaining with the oligodendrocyte marker receptor-interacting protein (RIP) showed that EphrinA3 is also expressed in oligodendrocytes (Fig. 2G and H). Single-cell densitometric quantification of EphrinA3 expression in the lumbar spinal cord at level L_4–L_6 (Fig. 2I) revealed its significant upregulation in both neurons and oligodendrocytes of Nogo-A KO mice (Fig. 2J). The upregulation of EphrinA3 in the gray matter was reflected by a marked increase in the analysed Rexed's laminae I–III (~54%; $t_4 = 3.479$, $P = 0.025$, $n = 3$), IV (~46%; $t_4 = 4.513$, $P = 0.011$, $n = 3$), VII (~56%; $t_4 = 2.711$, $P = 0.054$, $n = 3$) and IX (~71%; $t_4 = 3.308$, $P = 0.030$, $n = 3$; unpaired two-tailed Student's t test; Fig. 2J). In the white matter, EphrinA3 immunoreactivity in oligodendrocytes was increased by ~120% ($t_4 = 4.193$, $P = 0.014$, $n = 3$) and ~97% ($t_4 = 4.501$, $P = 0.011$, $n = 3$) in the dorsal and ventral funiculus, respectively (unpaired two-tailed Student's t test; Fig. 2J). The predominant upregulation of EphrinA3 in myelinating oligodendrocytes, coupled to the known axonal expression of EphA4 (Kullander *et al.*, 2001; Leighton *et al.*, 2001), suggested that myelin-associated EphrinA3 might restrict axonal growth and regeneration via EphA4 in the spinal cord of Nogo-A KO mice.

EphrinA3 inhibits neurite outgrowth via EphA4 in vitro

We investigated the growth-inhibitory properties of EphrinA3 by analysing the outgrowth of two neuronal cell types plated on a clustered EphrinA3-Fc substrate. P5–P8 WT cortical neurons, which endogenously express the EphA4 receptor (Fig. 3A; Benson *et al.*, 2005), were significantly inhibited by EphrinA3-Fc when compared with the Fc control ($t_{10} = 6.606$, $P < 0.001$, $n = 6$; unpaired two-tailed Student's t test; Fig. 3B and C). By contrast, P5–P8 DRG neurons, which do not express detectable levels of EphA4, were not significantly inhibited by EphrinA3-Fc ($P = 0.465$, $n = 3$; unpaired two-tailed Student's t test; Fig. 3A, D and E). To confirm the role of EphA4 for EphrinA3-mediated growth inhibition, cortical neurons were isolated from EphA4 KO mice and plated on clustered EphrinA3-Fc. Notably, EphA4 KO cortical neurons were not inhibited by EphrinA3-Fc when compared with control Fc ($P = 0.602$, $n = 6$; unpaired two-tailed Student's t test; Fig. 3B and C), showing that EphA4 mediates EphrinA3-induced growth inhibition.

We then addressed the inhibitory properties of membrane-enriched EphrinA3 KO spinal cord extracts on neurite outgrowth of cortical neurons. When compared with extracts prepared from WT and Nogo-A KO mice, we found that EphrinA3 KO extracts were significantly less inhibitory than WT ($t_{12} = 3.046$, $P = 0.011$, $n = 7$; unpaired two-tailed Student's t test) but more than Nogo-A KO extracts ($t_{12} = 2.234$, $P = 0.047$, $n = 7$; unpaired two-tailed Student's t test; Fig. 3F and G). Finally, we investigated whether EphA4 KO cortical neurons grown on Nogo-A KO spinal cord extracts would show a decreased inhibition as compared with WT neurons. Indeed, EphA4 KO cortical neurons were significantly less inhibited by Nogo-A KO spinal cord extracts than WT neurons ($t_{14} = 2.462$, $P = 0.026$, $n = 7$; unpaired two-tailed Student's t test; Fig. 3H and I). These results support a functional role for the broad-range Ephrin receptor EphA4 in mediating increased growth inhibition following constitutive Nogo-A ablation.

CST regeneration after spinal cord injury in WT, Nogo-A KO, EphA4 KO and Nogo-A/EphA4 double KO mice

Given the increased EphA4-mediated growth inhibition in Nogo-A KO mice, we reasoned that the combined deletion of Nogo-A and EphA4 may have an additive or synergistic effect on axonal regeneration. This was addressed by analysing axonal sprouting and regeneration following spinal cord injury in newly generated Nogo-A/EphA4 double KO mice. As described for EphA4 KO mice, also Nogo-A/EphA4 KO mice showed a majority of normally positioned CST axons within the dorsal funiculus but these axons had aberrant projections across the midline forming bilateral connections (Dottori *et al.*, 1998; Coonan *et al.*, 2001; Kullander *et al.*, 2001; Leighton *et al.*, 2001). In addition, Nogo-A/EphA4 KO mice showed a ventral displacement of the mature CST termination pattern reaching the intermediate zone of the spinal cord as described for EphA4 KO alone (Coonan *et al.*, 2001). Thus, the aberrant CST projections precluded a reliable comparison between EphA4-positive and -negative genotypes, especially in the zone of regenerative sprouting at the lesion site (surviving displaced CST axon branches could not be distinguished from sprouting fibers in the tissue bridge ventral to the lesion) and in the caudal spinal cord. Therefore, WT mice were compared with Nogo-A KO mice, and EphA4 KOs with Nogo-A/EphA4 KOs. Similar to EphA4 KO mice (Herrmann *et al.*, 2010b), Nogo-A/EphA4 double KO mice also showed pronounced balance problems manifested as lateral recumbency after spinal cord injury,

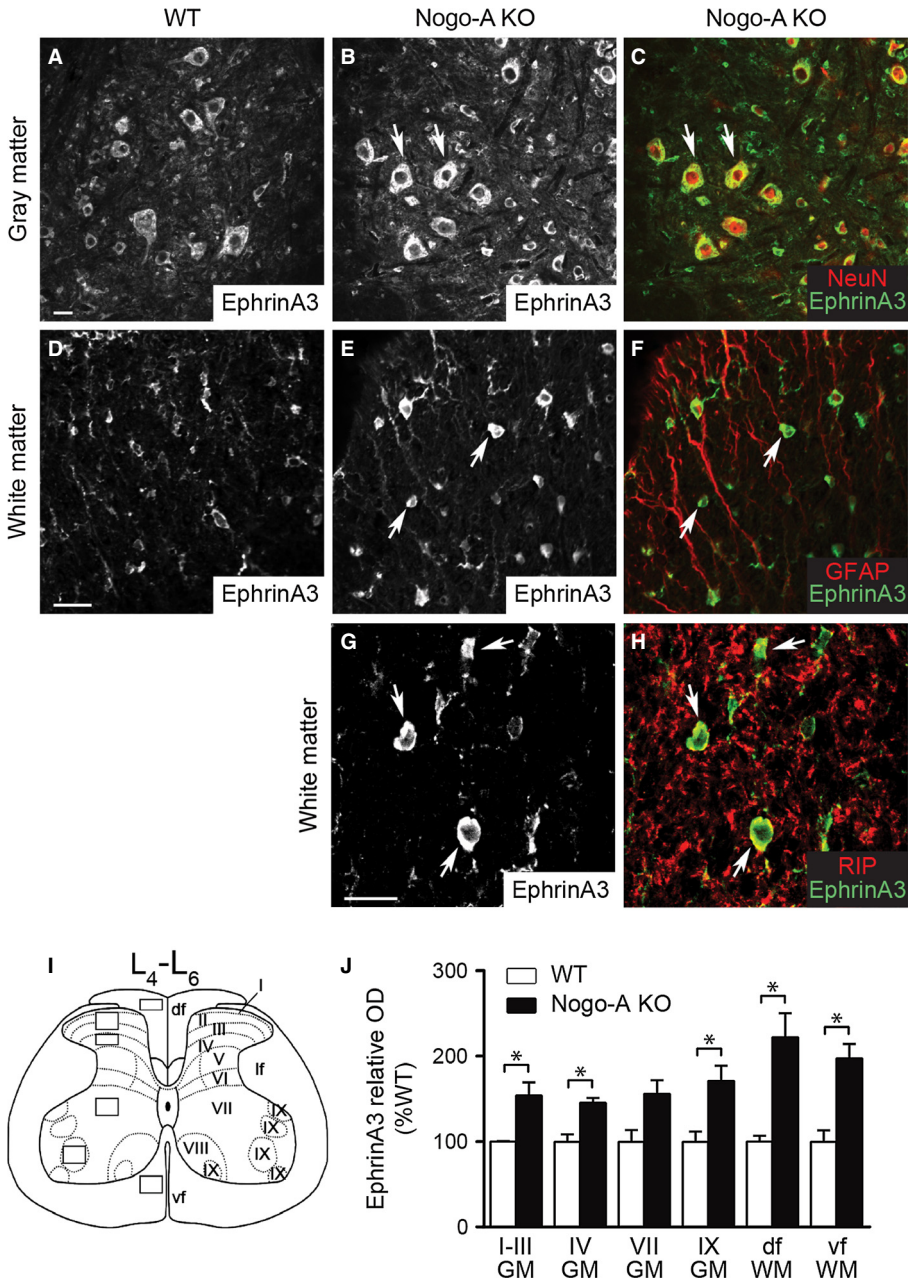

FIG. 2. EphrinA3 is upregulated in spinal cord neurons and oligodendrocytes of Nogo-A KO mice. (A–C) Immunohistochemical analysis of EphrinA3 expression in the lumbar spinal cord gray matter of WT (A) and Nogo-A KO mice (B) reveals the presence of EphrinA3 in NeuN-positive neurons (Lamina IX) (C). (D–F) Double immunostaining of EphrinA3 (D–F) and GFAP (F) in the lumbar spinal cord white matter (df) shows the lack of EphrinA3 expression in astrocytes. (G,H) Co-localization of EphrinA3 (G) with the oligodendrocyte marker RIP (H) reveals the presence of EphrinA3 in oligodendrocytes of Nogo-A KO mice. (I) Schematic drawing of a lumbar spinal cord cross-section illustrating the analysed regions (left) in the gray and white matter. (J) Single-cell densitometric quantification of EphrinA3 expression in NeuN-positive neurons in Laminae I–III, IV, VII and IX; and of RIP-positive oligodendrocytes in the dorsal (df) and ventral (vf) white matter. Ten cells were analysed per condition. Arrows indicate EphrinA3-positive cells in the Nogo-A KO spinal cord. Data shown are means ± SEM (n = 3 mice; *$P < 0.05$; Student's t test). GM = gray matter; WM = white matter; df = dorsal funiculus; vf = ventral funiculus; lf = lateral funiculus; Scale bars: 100 μm.

which made many behavioral tests difficult or impossible to perform.

In 20-weeks-old WT, Nogo-A KO, EphA4 KO and Nogo-A/EphA4 double KO mice, the dorsal half of the spinal cord, including the main CST and its minor components in the dorso-lateral funiculi, was transected bilaterally. The volume of the GFAP-negative lesion core was measured. No significant differences could be observed among the mice of different genotypes (WT: 0.067 ± 0.004 mm^3 (n = 6), Nogo-A KO: 0.055 ± 0.006 mm^3 (n = 10), EphA4 KO: 0.059 ± 0.006 mm^3 (n = 7), Nogo-A/EphA4 KO: 0.065 ± 0.004 mm^3 (n = 5); $F_{3,24} = 1.007$, $P = 0.406$; one-way ANOVA with Bonferroni's *post hoc* test) (Fig. 4A and B). In accordance with a previous study (Goldshmit *et al.*, 2004), the astrocytic scar volume, defined as GFAP-positive tissue volume surrounding the lesion core, was significantly smaller in EphA4 KO ($P < 0.01$) and Nogo-A/EphA4 double KO ($P < 0.05$), but not in Nogo-A KO mice when compared with WT mice (WT: 0.528 ± 0.059 mm^3 (n = 6), Nogo-A KO: 0.413 ± 0.061 mm^3 (n = 10), EphA4 KO:

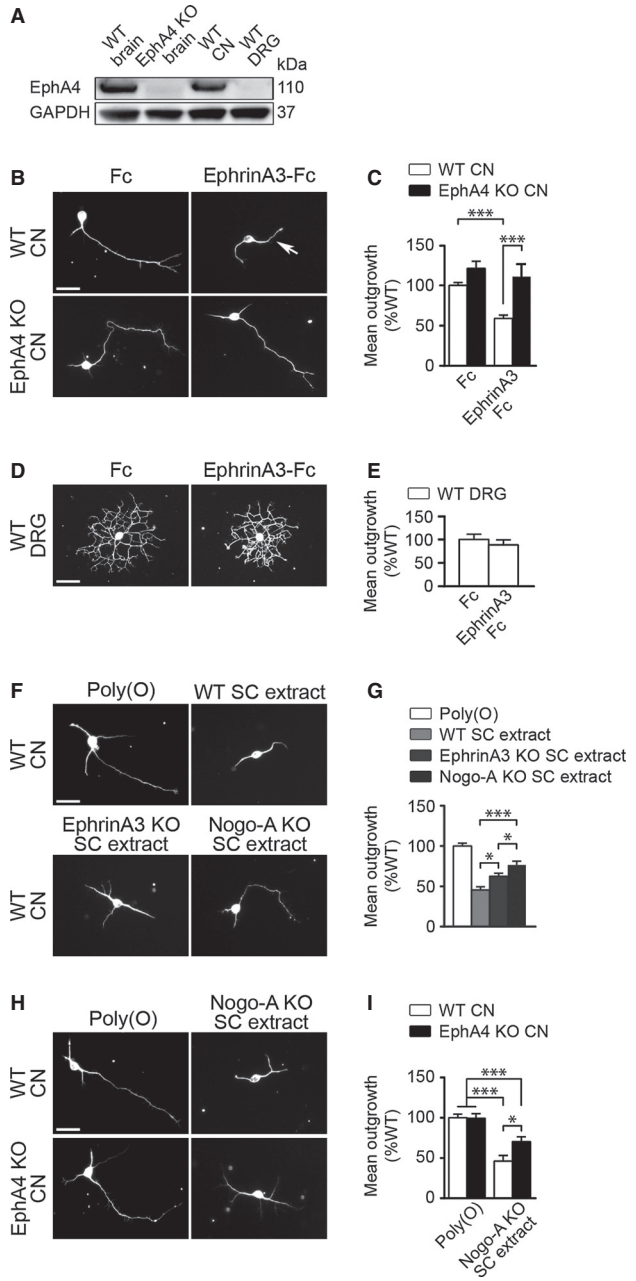

FIG. 3. EphrinA3 inhibits neurite outgrowth of cortical neurons (CNs) via EphA4 *in vitro*. (A) Western blot showing that EphA4 is expressed in WT P5–P8 dissociated CNs but not DRG neurons. WT and EphA4 KO brain tissue was used as positive and negative control, respectively. GAPDH was used as loading control. (B) Representative pictures of WT and EphA4 KO CNs cultured on a clustered Fc (control) or EphrinA3-Fc substrate (0.5 μg/cm^2). (C) Clustered EphrinA3-Fc inhibits neurite outgrowth of EphA4-positive WT CNs but not of EphA4 KO CNs. (D) Representative pictures of WT DRG neurons cultured on a clustered Fc (control) or EphrinA3-Fc substrate (0.5 μg/cm^2). (E) Clustered EphrinA3-Fc does not inhibit neurite outgrowth of DRG neurons. (F) Representative pictures of WT CNs plated on WT, EphrinA3 KO or Nogo-A KO membrane-enriched spinal cord extracts (6 μg/cm^2). Poly(O) was used as control. (G) EphrinA3 KO spinal cord extracts are significantly less inhibitory than WT but more than Nogo-A KO spinal cord extracts. (H) Representative images of WT and EphA4 KO CNs on Nogo-A KO spinal cord extracts. Poly(O) was used as control. (I) EphA4 KO CNs are significantly less inhibited than WT CNs by Nogo-A KO spinal cord extracts. Data shown are means ± SEM (n = 3–7 independent experiments; *P < 0.05, ***P < 0.001; Student's t test). In total, 150–200 cells were analysed per condition. CN = cortical neurons; DRG = dorsal root ganglia; SC = spinal cord. Scale bars: 50 μm.

0.189 ± 0.039 mm^3 (n = 7), Nogo-A/EphA4 KO: 0.313 ± 0.093 mm^3 (n = 5)) ($F_{3,24}$ = 7.245, P = 0.001; one-way ANOVA with Bonferroni's *post hoc* test; Fig. 4A and C).

Sprouting of CST axons 1 mm rostral to the lesion was assessed using a 0–3 point scoring scale. As previously described by Dimou *et al.* (2006), sprouting was moderate in WTs and significantly increased in Nogo-A KO mice (WT: 1.24 ± 0.18 n = 10, Nogo-A KO: 1.86 ± 0.21 n = 12; t_{13} = 2.604, P = 0.03; Welch's t test; Fig. 5A, A′, B and B′). In EphA4 KO and Nogo-A/EphA4 KO mice, sprouting was further increased but comparable between the genotypes (EphA4 KO: 2.20 ± 0.24, n = 11; Nogo-A/EphA4 KO: 2.33 ± 0.19, n = 9; t_{11} = 0.847, P = 0.69; Welch's t test; Fig. 5C, C′, D and D′). Many of these fibers extended laterally and ventrally from the main CST into the adjacent gray and white matter and below the lesion (Fig. 5A′–D′; arrows). In both EphA4 KO and Nogo-A/EphA4 double KO mice, many sprouts ended very close to or in the lesion itself (Fig. 5C′ and D′; arrowheads). Due to the aberrant ventral course of some CST fibers in the EphA4 KO spinal cord, an unknown proportion of the fibers curving around the lesion in the ventral tissue bridge in EphA4 KO and Nogo-A/EphA4 KOs may be intact spared CST fibers in addition to regenerating and sprouting fibers (Fig. 5E 'lesion site'). Nevertheless, the number of fibers that bypassed the lesion on the ventral tissue bridges was larger in Nogo-A KO and Nogo-A/EphA4 KO mice than in the respective controls. CST axons that were present in the spinal cord caudal to the lesion were quantified at 1, 3, 5 and 10 mm past the lesion (Dimou *et al.*, 2006). An irregular, tortuous and often branched growth pattern of thin fibers typical of regenerative growth was observed (Simonen *et al.*, 2003; Liebscher *et al.*, 2005; Fig. 5A″–D″). As previously described, Nogo-A KO mice showed a significant increase in the number of regenerating fibers at 1, 3 and 5 mm past the lesion when compared with WT mice (Fig. 5E; Simonen *et al.*, 2003; Dimou *et al.*, 2006). EphA4 KO mice displayed more fibers than WT and Nogo-A KO mice up to 10 mm caudal to the lesion, even though these fibers probably represent a mixture of regenerated axons and branches/sprouts of spared axons (see above; Fig. 5E). These results support previous evidence for a role of EphA4 in restricting axonal regeneration in the adult CNS (Goldshmit *et al.*, 2004, 2011) and suggest that Nogo-A and EphA4 may additively restrict axonal sprouting and regeneration in the adult CNS.

Discussion

We performed mRNA expression profiling of the intact spinal cord of adult constitutive C57BL/6 Nogo-A KO (Simonen *et al.*, 2003; Dimou *et al.*, 2006) vs. WT mice to identify compensatory alterations that may account for residual growth inhibition in the absence of Nogo-A. Our study shows that the repulsive axon guidance molecules Sema4D, Sema3F, EphrinA3 and EphA4 are upregulated in the adult spinal cord of Nogo-A KO mice at transcript and protein level. We identify EphrinA3 as a novel, myelin-associated inhibitor of neurite outgrowth in the adult CNS and we find EphA4-mediated growth inhibition upregulated in Nogo-A KO mice. *In vivo*, we confirm a role for EphA4 in restricting axonal regeneration in the adult CNS and show that combined deletion of Nogo-A and EphA4 results in increased regenerative growth after spinal cord injury when compared with EphA4 KO mice.

EphrinA3 has been known mainly for its role in synaptic remodeling and plasticity in the hippocampus (Pasquale, 2005). Here we show that EphrinA3 is also expressed in adult white matter oligodendrocytes and inhibits neurite outgrowth of primary neurons in an EphA4-dependent manner *in vitro*. The upregulation of three major

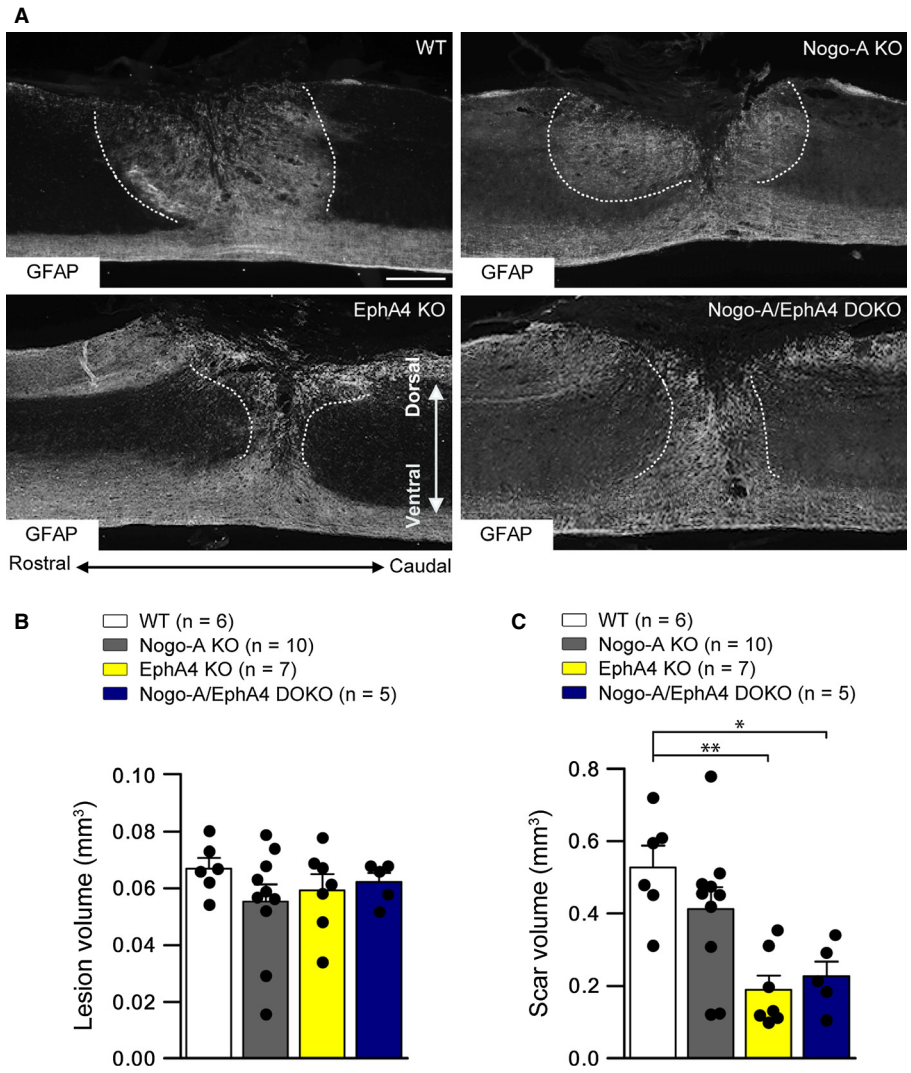

FIG. 4. Astrocytic glyosis is diminished in mice lacking EphA4. (A) Representative images of spinal cord mid-sagittal sections from WT, Nogo-A KO, EphA4 KO and Nogo-A/EphA4 KO mice showing GFAP immunoreactivity around the lesion site 24 days after spinal cord lesion. (B) Quantification of lesion-induced tissue damage expressed as lesion volume, which is defined as the GFAP-negative region of the lesion core. Lesion volume was comparable between mice of all four genotypes. (C) Quantification of astrocytic gliosis expressed as scar tissue volume. The scar area was defined as the GFAP-positive region surrounding the lesion core. Gliotic scarring was reduced in EphA4 KO and Nogo-A/EphA4 KO after spinal cord injury. Dotted line outlines the GFAP-immunopositive scar area. Data shown are means ± SEM (n = 5–10 mice; $^*P < 0.05$, $^{**}P < 0.01$; one-way ANOVA followed by Bonferroni's *post hoc* test). DOKO = double KO. Scale bar: 300 μm.

Cdk5 regulators (p35-Cdk5, Cables1 and Fnbp2/Cdkrap2), previously implicated in dendritic spine retraction upon EphrinA3-induced activation of EphA4 in the hippocampus (Zukerberg *et al.*, 2000; Fu *et al.*, 2007), suggests that Cdk5 might be a key downstream mediator of the EphrinA3/EphA4 inhibitory pathway. Further studies will be needed to further address the role of Cdk5 in neurite outgrowth inhibition. A chemorepellent function has also been previously attributed to Sema3F and Sema4D in the injured CNS and scar tissue (Pasterkamp & Verhaagen, 2006). Sema4D is expressed in oligodendrocytes, upregulated after CNS injury, and inhibits the growth of postnatal sensory and cerebellar granule cell neurons *in vitro* (Moreau-Fauvarque *et al.*, 2003). Sema3F is secreted into the glial-fibrotic scar by meningeal fibroblasts (Pasterkamp *et al.*, 1999; De Winter *et al.*, 2002), upregulated after intraspinal motoneuron axotomy (Lindholm *et al.*, 2004) and induces growth cone collapse *in vitro* (Atwal *et al.*, 2003). Together, these changes indicate that Sema4D, Sema3F and EphrinA3 may also impact the regenerative response observed in Nogo-A KO mice. Their relative functional contributions remain to be determined. It would be of particular interest to know whether similar compensatory changes also occur in other targeted and gene trap Nogo mutants and how closely they are associated with the observed, line-specific regenerative phenotypes. Variations in the degree of upregulation of compensatory mechanisms could play an important role for the observed differential growth and regeneration capacity in the different Nogo-A, Nogo-A/B and Nogo-A/B/C KO lines (Kim *et al.*, 2003; Simonen *et al.*, 2003; Zheng *et al.*, 2003; Cafferty & Strittmatter, 2006; Dimou *et al.*, 2006; Lee *et al.*, 2009).

Our results point to a functional role for the broad-range Ephrin receptor EphA4 in mediating growth-restricting signals in Nogo-A KO mice. By using a dorsal bilateral hemisection spinal cord injury model, we specifically assessed a potential additive or synergistic role of Nogo-A and of EphA4 in axonal regeneration. It is of note that signaling pathways induced by Nogo-A and EphA4 converge

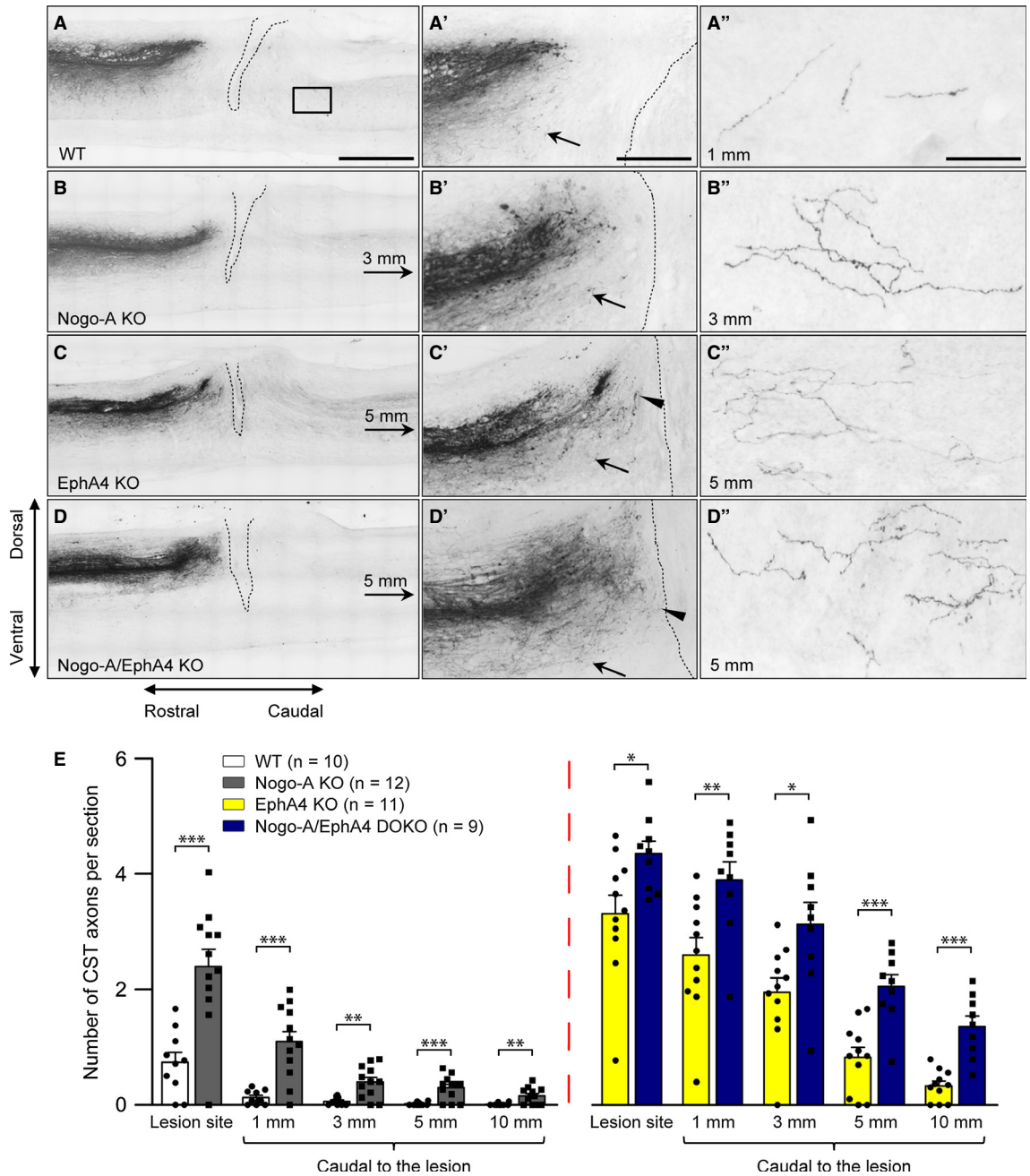

FIG. 5. Sprouting and long-distance regeneration of CST axons in WT, Nogo-A KO, EphA4 KO and Nogo-A/EphA4 double KO mice. (A–D) Representative images of BDA-labeled CST axons in sagittal sections of the thoracic spinal cord after dorsal hemisection (delineated by dotted lines) in WT (A), Nogo-A KO (B), EphA4 KO (C) and Nogo-A/EphA4 DOKO (D) mice. Higher-magnification views immediately rostral to the lesion site (A′–D′) illustrate enhanced sprouting and reduced CST retraction from the lesion site in mutant mice. Numerous sprouting fibers extended laterally and ventrally from the main CST into the adjacent gray and white matter (arrows). In EphA4 KO mice, fiber sprouts ended very close to the lesion edge (arrowheads). High-magnification views caudal to the injury (A″–D″) and corresponding to the marked regions in A–D illustrate regenerating CST fibers extending past the lesion site. (E) Quantification of the number of BDA-labeled CST axons in the lesion center and at 1, 3, 5 and 10 mm caudal to the lesion. Nogo-A KO mice exhibited significantly more CST axons at the lesion site and up to 10 mm caudal to the lesion site. Regenerative sprouting and long-distance regeneration is significantly increased in Nogo-A/EphA4 DOKO compared with single EphA4 KO mice. CST axon guidance defects in EphA4 KO and Nogo-A/EphA4 DOKO mice, which include an increased number of ventrally misplaced fibers, precluded a reliable direct statistical comparison between EphA4-negative genotypes and WT or Nogo-A KO mice. Data shown are means ± SEM (n = 9–12 mice; *$P < 0.05$, **$P < 0.01$, ***$P < 0.001$; Welch's t test). DOKO = double KO. Scale bars: 1 mm (A–D), 500 μm (A′–D′) and 50 μm (A″–D″).

towards the activation of the small GTPase RhoA, which is central to growth repulsion and inhibition of axonal regeneration (Pasquale, 2005; Schwab, 2010). In line with previous studies (Goldshmit *et al.*, 2004; Dimou *et al.*, 2006), we observed a significantly larger number of sprouting and regenerating fibers in single Nogo-A KO and EphA4 KO mice rostral and caudal to the lesion site, respectively, which was augmented in Nogo-A/EphA4 double KO mice. These results suggest an additive role for Nogo-A and EphA4 in restricting axonal regeneration post-injury. However, despite strict quantification criteria, it is possible that an unknown proportion of

ventrally misplaced CST axons, inappropriately terminating within the intermediate zone of the spinal cord, escaped the lesion in EphA4 KO and Nogo-A/EphA4 KO mice. Fibers caudal to the lesion might thus be a mixture of regenerating and spared, sprouting fibers in these mutants. For this reason, cross-comparisons of EphA4 KO and Nogo-A/EphA4 KO mice with WT or Nogo-A single KO mice could not be made and were not included in the analysis. Importantly, these fibers do not arise from a different neuronal subpopulation but their misplacement is rather due to an axonal guidance defect of the developing CST (Coonan *et al.*, 2001). Further studies using inducible conditional EphA4 KO mice without major developmental defects will allow further clarifying the functional role of EphA4 in axonal regeneration (Herrmann *et al.*, 2010a).

EphA4 is expressed in astrocytes and neurons (including CST axons) of the adult spinal cord (Kullander *et al.*, 2001; Leighton *et al.*, 2001; Goldshmit *et al.*, 2004; Herrmann *et al.*, 2010b) and is upregulated after spinal cord injury (Goldshmit *et al.*, 2004; Fabes *et al.*, 2006). Previous studies showed that genetic deletion or functional blockade of EphA4 using soluble ligands or receptors resulted in enhanced axonal sprouting and in a variable degree of regeneration and functional recovery 6 weeks after a spinal cord lesion *in vivo* (Goldshmit *et al.*, 2004, 2011; Cruz-Orengo *et al.*, 2007; Fabes *et al.*, 2007). The mechanisms by which EphA4 modulates axonal regeneration are probably complex given its ligand-binding promiscuity, its expression pattern and the occurrence of Ephrin/Eph bidirectional signaling (Klein, 2009). EphA4 binds multiple EphrinA and EphrinB ligand subtypes, thereby enabling a variety of molecular and intercellular interactions (Pasquale, 2005). Activation of axonal EphA4 by Ephrin ligands expressed on astrocytes and/or on myelin such as EphrinB2 and EphrinB3 has been proposed to result in growth cone collapse via the Ephexin1/RhoA pathway (Shamah *et al.*, 2001; Bundesen *et al.*, 2003; Benson *et al.*, 2005; Sahin *et al.*, 2005). *In vivo*, genetic deletion of EphrinB3 resulted in increased axonal regeneration and functional recovery after a dorsal hemisection spinal cord lesion, suggesting that EphrinB3 also contributes to the myelin-dependent inhibition of axonal regeneration (Duffy *et al.*, 2012). In addition, Ephrins expressed in axonal growth cones may also induce growth cone collapse upon contact with astrocytic EphA4 via reverse signaling (Goldshmit *et al.*, 2004). A different mechanism may also be the modulation of the neuroinflammatory response in EphA4 KO mice after spinal cord injury (Munro *et al.*, 2012).

Goldshmit *et al.* (2004) reported decreased astrocyte reactivity in the scar area as an additional mechanism that could positively influence regenerative fiber growth in EphA4 KO mice as opposed to a similar study by Herrmann *et al.* (2010b). We obtained similar results to those of Goldshmit *et al.* (2004) in our EphA4 KO and Nogo-A/EphA4 double KO mice, indicating that increased regeneration at the lesion site might rely on a reduction in astrocytic gliosis as well as on reduced levels of and decreased axonal sensitivity to myelin-associated inhibitors. In Nogo-A KO mice, astrocytic gliosis was not affected, suggesting that the increased number of CST fibers caudal to the lesion site are most likely the result of a reduced myelin-mediated growth inhibition by genetic removal of Nogo-A.

In summary, our results show the upregulation of several known repellent axon guidance family members and of their receptors in the adult CNS of Nogo-A KO mice. In the injured spinal cord, these molecules, e.g. EphrinA3/EphA4, impede axonal regeneration and their upregulation may partially account for the retained inhibitory properties observed in Nogo-A KO mice. Their modulation was detectable in the intact adult spinal cord, further suggesting that these upregulated repulsive cues may not only counteract regeneration following a lesion, but also contribute to the growth- and plasticity-restricting, circuit-stabilizing function attributed to Nogo-A in the adult CNS (Schwab, 2010; Akbik *et al.*, 2012). Further studies will be key to further clarify their specific role in this context.

Supporting Information

Additional supporting information can be found in the online version of this article:
Table S1. Differentially expressed transcripts in the spinal cord of Nogo-A KO vs. WT mice

Acknowledgements

This work was supported by grants of the Swiss National Science Foundation (SNF; 3100A0-122527/1 and 310030B-138676/1), the NCCR 'Neural Plasticity and Repair' of the SNF, and the Spinal Cord Consortium of the Christopher and Dana Reeve Foundation (Springfield, NJ, USA). We thank R. Klein (Max-Planck Institute for Neurobiology, Martinsried, Germany) for providing EphA4 KO mice and D. Feldheim (University of California, Santa Cruz, CA, USA) for supplying EphrinA3 KO tissue. We thank F. Christ, M. Gullo and R. Schneider for excellent technical help, and M. Kuenzli and U. Wagner of the Functional Genomic Center of Zurich for valuable advices and practical help on the GeneChip experimental setup and data analysis. We thank F. Verrey (Institute of Physiology, University of Zurich, Switzerland) for providing access to the Applied Biosystem qRT-PCR system, A. Bruns for helping with the statistical analysis, and L. Bachmann, M. Arzt and V. Pernet for critical reading of the manuscript. The authors declare no competing financial interests.

Abbreviations

ANOVA, analysis of variance; BDA, biotin dextran amine; CNS, central nervous system; CST, corticospinal tract; DAB, diaminobenzidine; DRG, dorsal root ganglia; GADPH, glyceraldehyde-3-phosphate dehydrogenase; GFAP, glial fibrillary acidic protein; IHC, immunohistochemistry; KO, knockout; MAG, myelin-associated glycoprotein; OMgp, oligodendrocyte myelin glycoprotein; PB, phosphate buffer; PBS, phosphate-buffered saline; PFA, paraformaldehyde; PLL, poly-L-lysine; PMSF, phenylmethanesulfonyl fluoride; qRT-PCR, quantitative real-time PCR; RIP, receptor interacting protein; SEM, standard error of the mean; WB, Western blot.

References

Akbik, F., Cafferty, W.B. & Strittmatter, S.M. (2012) Myelin associated inhibitors: a link between injury-induced and experience-dependent plasticity. *Exp. Neurol.*, **235**, 43–52.

Atwal, J.K., Singh, K.K., Tessier-Lavigne, M., Miller, F.D. & Kaplan, D.R. (2003) Semaphorin 3F antagonizes neurotrophin-induced phosphatidylinositol 3-kinase and mitogen-activated protein kinase kinase signaling: a mechanism for growth cone collapse. *J. Neurosci.*, **23**, 7602–7609.

Benson, M.D., Romero, M.I., Lush, M.E., Lu, Q.R., Henkemeyer, M. & Parada, L.F. (2005) Ephrin-B3 is a myelin-based inhibitor of neurite outgrowth. *Proc. Natl. Acad. Sci. USA*, **102**, 10694–10699.

Bradbury, E.J., Moon, L.D., Popat, R.J., King, V.R., Bennett, G.S., Patel, P.N., Fawcett, J.W. & McMahon, S.B. (2002) Chondroitinase ABC promotes functional recovery after spinal cord injury. *Nature*, **416**, 636–640.

Buchli, A.D., Rouiller, E., Mueller, R., Dietz, V. & Schwab, M.E. (2007) Repair of the injured spinal cord. A joint approach of basic and clinical research. *Neurodegener. Dis.*, **4**, 51–56.

Bundesen, L.Q., Scheel, T.A., Bregman, B.S. & Kromer, L.F. (2003) Ephrin-B2 and EphB2 regulation of astrocyte-meningeal fibroblast interactions in response to spinal cord lesions in adult rats. *J. Neurosci.*, **23**, 7789–7800.

Cafferty, W.B. & Strittmatter, S.M. (2006) The Nogo-Nogo receptor pathway limits a spectrum of adult CNS axonal growth. *J. Neurosci.*, **26**, 12242–12250.

Cafferty, W.B., Duffy, P., Huebner, E. & Strittmatter, S.M. (2010) MAG and OMgp synergize with Nogo-A to restrict axonal growth and neurological recovery after spinal cord trauma. *J. Neurosci.*, **30**, 6825–6837.

Chen, M.S., Huber, A.B., van der Haar, M.E., Frank, M., Schnell, L., Spillmann, A.A., Christ, F. & Schwab, M.E. (2000) Nogo-A is a myelin-associated neurite outgrowth inhibitor and an antigen for monoclonal antibody IN-1. *Nature*, **403**, 434–439.

Coonan, J.R., Greferath, U., Messenger, J., Hartley, L., Murphy, M., Boyd, A.W., Dottori, M., Galea, M.P. & Bartlett, P.F. (2001) Development and reorganization of corticospinal projections in EphA4 deficient mice. *J. Comp. Neurol.*, **436**, 248–262.

Craveiro, L.M., Hakkoum, D., Weinmann, O., Montani, L., Stoppini, L. & Schwab, M.E. (2008) Neutralization of the membrane protein Nogo-A enhances growth and reactive sprouting in established organotypic hippocampal slice cultures. *Eur. J. Neurosci.*, **28**, 1808–1824.

Cruz-Orengo, L., Figueroa, J.D., Velazquez, I., Torrado, A., Ortiz, C., Hernandez, C., Puig, A., Segarra, A.C., Whittemore, S.R. & Miranda, J.D. (2006) Blocking EphA4 upregulation after spinal cord injury results in enhanced chronic pain. *Exp. Neurol.*, **202**, 421–433.

Cruz-Orengo, L., Figueroa, J.D., Torrado, A., Puig, A., Whittemore, S.R. & Miranda, J.D. (2007) Reduction of EphA4 receptor expression after spinal cord injury does not induce axonal regeneration or return of tcMMEP response. *Neurosci. Lett.*, **418**, 49–54.

Cutforth, T., Moring, L., Mendelsohn, M., Nemes, A., Shah, N.M., Kim, M.M., Frisen, J. & Axel, R. (2003) Axonal ephrin-As and odorant receptors: coordinate determination of the olfactory sensory map. *Cell*, **114**, 311–322.

De Winter, F., Oudega, M., Lankhorst, A.J., Hamers, F.P., Blits, B., Ruitenberg, M.J., Pasterkamp, R.J., Gispen, W.H. & Verhaagen, J. (2002) Injury-induced class 3 semaphorin expression in the rat spinal cord. *Exp. Neurol.*, **175**, 61–75.

Dimou, L., Schnell, L., Montani, L., Duncan, C., Simonen, M., Schneider, R., Liebscher, T., Gullo, M. & Schwab, M.E. (2006) Nogo-A-deficient mice reveal strain-dependent differences in axonal regeneration. *J. Neurosci.*, **26**, 5591–5603.

Dottori, M., Hartley, L., Galea, M., Paxinos, G., Polizzotto, M., Kilpatrick, T., Bartlett, P.F., Murphy, M., Kontgen, F. & Boyd, A.W. (1998) EphA4 (Sek1) receptor tyrosine kinase is required for the development of the corticospinal tract. *Proc. Natl. Acad. Sci. USA*, **95**, 13248–13253.

Duffy, P., Wang, X., Seigel, C.S., Tu, N., Henkemeyer, M., Cafferty, W.B. & Strittmatter, S.M. (2012) Myelin-derived ephrinB3 restricts axonal regeneration and recovery after adult CNS injury. *Proc. Natl. Acad. Sci. USA*, **109**, 5063–5068.

Fabes, J., Anderson, P., Yanez-Munoz, R.J., Thrasher, A., Brennan, C. & Bolsover, S. (2006) Accumulation of the inhibitory receptor EphA4 may prevent regeneration of corticospinal tract axons following lesion. *Eur. J. Neurosci.*, **23**, 1721–1730.

Fabes, J., Anderson, P., Brennan, C. & Bolsover, S. (2007) Regeneration-enhancing effects of EphA4 blocking peptide following corticospinal tract injury in adult rat spinal cord. *Eur. J. Neurosci.*, **26**, 2496–2505.

Fawcett, J.W. (2006) The glial response to injury and its role in the inhibition of CNS repair. *Adv. Exp. Med. Biol.*, **557**, 11–24.

Fu, W.Y., Chen, Y., Sahin, M., Zhao, X.S., Shi, L., Bikoff, J.B., Lai, K.O., Yung, W.H., Fu, A.K., Greenberg, M.E. & Ip, N.Y. (2007) Cdk5 regulates EphA4-mediated dendritic spine retraction through an ephexin1-dependent mechanism. *Nat. Neurosci.*, **10**, 67–76.

Goldberg, J.L., Vargas, M.E., Wang, J.T., Mandemakers, W., Oster, S.F., Sretavan, D.W. & Barres, B.A. (2004) An oligodendrocyte lineage-specific semaphorin, Sema5A, inhibits axon growth by retinal ganglion cells. *J. Neurosci.*, **24**, 4989–4999.

Goldshmit, Y., Galea, M.P., Wise, G., Bartlett, P.F. & Turnley, A.M. (2004) Axonal regeneration and lack of astrocytic gliosis in EphA4-deficient mice. *J. Neurosci.*, **24**, 10064–10073.

Goldshmit, Y., Spanevello, M.D., Tajouri, S., Li, L., Rogers, F., Pearse, M., Galea, M., Bartlett, P.F., Boyd, A.W. & Turnley, A.M. (2011) EphA4 blockers promote axonal regeneration and functional recovery following spinal cord injury in mice. *PLoS ONE*, **6**, e24636.

GrandPre, T., Nakamura, F., Vartanian, T. & Strittmatter, S.M. (2000) Identification of the Nogo inhibitor of axon regeneration as a Reticulon protein. *Nature*, **403**, 439–444.

Hata, K., Fujitani, M., Yasuda, Y., Doya, H., Saito, T., Yamagishi, S., Mueller, B.K. & Yamashita, T. (2006) RGMa inhibition promotes axonal growth and recovery after spinal cord injury. *J. Cell Biol.*, **173**, 47–58.

Herrmann, J.E., Pence, M.A., Shapera, E.A., Shah, R.R., Geoffroy, C.G. & Zheng, B. (2010a) Generation of an EphA4 conditional allele in mice. *Genesis*, **48**, 101–105.

Herrmann, J.E., Shah, R.R., Chan, A.F. & Zheng, B. (2010b) EphA4 deficient mice maintain astroglial-fibrotic scar formation after spinal cord injury. *Exp. Neurol.*, **223**, 582–598.

Herzog, A. & Brosamle, C. (1997) 'Semifree-floating' treatment: a simple and fast method to process consecutive sections for immunohistochemistry and neuronal tracing. *J. Neurosci. Meth.*, **72**, 57–63.

Joset, A., Dodd, D.A., Halegoua, S. & Schwab, M.E. (2010) Pincher-generated Nogo-A endosomes mediate growth cone collapse and retrograde signaling. *Cell*, **188**, 271–285.

Kaneko, S., Iwanami, A., Nakamura, M., Kishino, A., Kikuchi, K., Shibata, S., Okano, H.J., Ikegami, T., Moriya, A., Konishi, O., Nakayama, C., Kumagai, K., Kimura, T., Sato, Y., Goshima, Y., Taniguchi, M., Ito, M., He, Z., Toyama, Y. & Okano, H. (2006) A selective Sema3A inhibitor enhances regenerative responses and functional recovery of the injured spinal cord. *Nat. Med.*, **12**, 1380–1389.

Kim, J.E., Li, S., GrandPre, T., Qiu, D. & Strittmatter, S.M. (2003) Axon regeneration in young adult mice lacking Nogo-A/B. *Neuron*, **38**, 187–199.

Klein, R. (2009) Bidirectional modulation of synaptic functions by Eph/ephrin signaling. *Nat. Neurosci.*, **12**, 15–20.

Kullander, K., Mather, N.K., Diella, F., Dottori, M., Boyd, A.W. & Klein, R. (2001) Kinase-dependent and kinase-independent functions of EphA4 receptors in major axon tract formation in vivo. *Neuron*, **29**, 73–84.

Lee, J.K. & Zheng, B. (2012) Role of myelin-associated inhibitors in axonal repair after spinal cord injury. *Exp. Neurol.*, **235**, 33–42.

Lee, J.K., Chan, A.F., Luu, S.M., Zhu, Y., Ho, C., Tessier-Lavigne, M. & Zheng, B. (2009) Reassessment of corticospinal tract regeneration in Nogo-deficient mice. *J. Neurosci.*, **29**, 8649–8654.

Lee, J.K., Geoffroy, C.G., Chan, A.F., Tolentino, K.E., Crawford, M.J., Leal, M.A., Kang, B. & Zheng, B. (2010) Assessing spinal axon regeneration and sprouting in Nogo-, MAG-, and OMgp-deficient mice. *Neuron*, **66**, 663–670.

Leighton, P.A., Mitchell, K.J., Goodrich, L.V., Lu, X., Pinson, K., Scherz, P., Skarnes, W.C. & Tessier-Lavigne, M. (2001) Defining brain wiring patterns and mechanisms through gene trapping in mice. *Nature*, **410**, 174–179.

Liebscher, T., Schnell, L., Schnell, D., Scholl, J., Schneider, R., Gullo, M., Fouad, K., Mir, A., Rausch, M., Kindler, D., Hamers, F.P. & Schwab, M.E. (2005) Nogo-A antibody improves regeneration and locomotion of spinal cord-injured rats. *Ann. Neurol.*, **58**, 706–719.

Lindholm, T., Skold, M.K., Suneson, A., Carlstedt, T., Cullheim, S. & Risling, M. (2004) Semaphorin and neuropilin expression in motoneurons after intraspinal motoneuron axotomy. *NeuroReport*, **15**, 649–654.

Liu, X., Hawkes, E., Ishimaru, T., Tran, T. & Sretavan, D.W. (2006) EphB3: an endogenous mediator of adult axonal plasticity and regrowth after CNS injury. *J. Neurosci.*, **26**, 3087–3101.

Low, K., Culbertson, M., Bradke, F., Tessier-Lavigne, M. & Tuszynski, M.H. (2008) Netrin-1 is a novel myelin-associated inhibitor to axon growth. *J. Neurosci.*, **28**, 1099–1108.

McKerracher, L., David, S., Jackson, D.L., Kottis, V., Dunn, R.J. & Braun, P.E. (1994) Identification of myelin-associated glycoprotein as a major myelin-derived inhibitor of neurite growth. *Neuron*, **13**, 805–811.

Montani, L., Gerrits, B., Gehrig, P., Kempf, A., Dimou, L., Wollscheid, B. & Schwab, M.E. (2009) Neuronal Nogo-A modulates growth cone motility via Rho-GTP/LIMK1/cofilin in the unlesioned adult nervous system. *J. Biol. Chem.*, **284**, 10793–10807.

Montolio, M., Messeguer, J., Masip, I., Guijarro, P., Gavin, R., Antonio Del Rio, J., Messeguer, A. & Soriano, E. (2009) A semaphorin 3A inhibitor blocks axonal chemorepulsion and enhances axon regeneration. *Chem. Biol.*, **16**, 691–701.

Moreau-Fauvarque, C., Kumanogoh, A., Camand, E., Jaillard, C., Barbin, G., Boquet, I., Love, C., Jones, E.Y., Kikutani, H., Lubetzki, C., Dusart, I. & Chedotal, A. (2003) The transmembrane semaphorin Sema4D/CD100, an inhibitor of axonal growth, is expressed on oligodendrocytes and upregulated after CNS lesion. *J. Neurosci.*, **23**, 9229–9239.

Mukhopadhyay, G., Doherty, P., Walsh, F.S., Crocker, P.R. & Filbin, M.T. (1994) A novel role for myelin-associated glycoprotein as an inhibitor of axonal regeneration. *Neuron*, **13**, 757–767.

Muller, P.Y., Janovjak, H., Miserez, A.R. & Dobbie, Z. (2002) Processing of gene expression data generated by quantitative real-time RT-PCR. *Biotechniques*, **32**, 1372–1374, 1376, 1378-1379.

Munro, K.M., Perreau, V.M. & Turnley, A.M. (2012) Differential gene expression in the EphA4 knockout spinal cord and analysis of the inflammatory response following spinal cord injury. *PLoS ONE*, **7**, e37635.

Oertle, T., van der Haar, M.E., Bandtlow, C.E., Robeva, A., Burfeind, P., Buss, A., Huber, A.B., Simonen, M., Schnell, L., Brosamle, C., Kaupmann, K., Vallon, R. & Schwab, M.E. (2003) Nogo-A inhibits neurite out-

growth and cell spreading with three discrete regions. *J. Neurosci.*, **23**, 5393–5406.
Park, K.K., Liu, K., Hu, Y., Smith, P.D., Wang, C., Cai, B., Xu, B., Connolly, L., Kramvis, I., Sahin, M. & He, Z. (2008) Promoting axon regeneration in the adult CNS by modulation of the PTEN/mTOR pathway. *Science*, **322**, 963–966.
Pasquale, E.B. (2005) Eph receptor signalling casts a wide net on cell behaviour. *Nat. Rev. Mol. Cell Biol.*, **6**, 462–475.
Pasterkamp, R.J. & Verhaagen, J. (2006) Semaphorins in axon regeneration: developmental guidance molecules gone wrong? *Philos. T. Roy. Soc. B*, **361**, 1499–1511.
Pasterkamp, R.J., Giger, R.J., Ruitenberg, M.J., Holtmaat, A.J., De Wit, J., De Winter, F. & Verhaagen, J. (1999) Expression of the gene encoding the chemorepellent semaphorin III is induced in the fibroblast component of neural scar tissue formed following injuries of adult but not neonatal CNS. *Mol. Cell. Neurosci.*, **13**, 143–166.
Prinjha, R., Moore, S.E., Vinson, M., Blake, S., Morrow, R., Christie, G., Michalovich, D., Simmons, D.L. & Walsh, F.S. (2000) Inhibitor of neurite outgrowth in humans. *Nature*, **403**, 383–384.
Sahin, M., Greer, P.L., Lin, M.Z., Poucher, H., Eberhart, J., Schmidt, S., Wright, T.M., Shamah, S.M., O'Connell, S., Cowan, C.W., Hu, L., Goldberg, J.L., Debant, A., Corfas, G., Krull, C.E. & Greenberg, M.E. (2005) Eph-dependent tyrosine phosphorylation of ephexin1 modulates growth cone collapse. *Neuron*, **46**, 191–204.
Schwab, M.E. (2004) Nogo and axon regeneration. *Curr. Opin. Neurobiol.*, **14**, 118–124.
Schwab, M.E. (2010) Functions of Nogo proteins and their receptors in the nervous system. *Nat. Rev. Neurosci.*, **11**, 799–811.
Shamah, S.M., Lin, M.Z., Goldberg, J.L., Estrach, S., Sahin, M., Hu, L., Bazalakova, M., Neve, R.L., Corfas, G., Debant, A. & Greenberg, M.E. (2001) EphA receptors regulate growth cone dynamics through the novel guanine nucleotide exchange factor ephexin. *Cell*, **105**, 233–244.
Shim, S.O., Cafferty, W.B., Schmidt, E.C., Kim, B.G., Fujisawa, H. & Strittmatter, S.M. (2012) PlexinA2 limits recovery from corticospinal axotomy by mediating oligodendrocyte-derived Sema6A growth inhibition. *Mol. Cell. Neurosci.*, **50**, 193–200.
Simonen, M., Pedersen, V., Weinmann, O., Schnell, L., Buss, A., Ledermann, B., Christ, F., Sansig, G., van der Putten, H. & Schwab, M.E. (2003) Systemic deletion of the myelin-associated outgrowth inhibitor Nogo-A improves regenerative and plastic responses after spinal cord injury. *Neuron*, **38**, 201–211.
Tews, B., Schonig, K., Arzt, M.E., Clementi, S., Rioult-Pedotti, M.S., Zemmar, A., Berger, S.M., Schneider, M., Enkel, T., Weinmann, O., Kasper, H., Schwab, M.E. & Bartsch, D. (2013) Synthetic microRNA-mediated downregulation of Nogo-A in transgenic rats reveals its role as regulator of synaptic plasticity and cognitive function. *Proc. Natl. Acad. Sci. USA*, **110**, 6583–6588.
Wang, K.C., Koprivica, V., Kim, J.A., Sivasankaran, R., Guo, Y., Neve, R.L. & He, Z. (2002) Oligodendrocyte-myelin glycoprotein is a Nogo receptor ligand that inhibits neurite outgrowth. *Nature*, **417**, 941–944.
Winzeler, A.M., Mandemakers, W.J., Sun, M.Z., Stafford, M., Phillips, C.T. & Barres, B.A. (2011) The lipid sulfatide is a novel myelin-associated inhibitor of CNS axon outgrowth. *J. Neurosci.*, **31**, 6481–6492.
Yiu, G. & He, Z. (2006) Glial inhibition of CNS axon regeneration. *Nat. Rev. Neurosci.*, **7**, 617–627.
Zheng, B., Ho, C., Li, S., Keirstead, H., Steward, O. & Tessier-Lavigne, M. (2003) Lack of enhanced spinal regeneration in Nogo-deficient mice. *Neuron*, **38**, 213–224.
Zorner, B. & Schwab, M.E. (2010) Anti-Nogo on the go: from animal models to a clinical trial. *Ann. NY Acad. Sci.*, **1198**(Suppl. 1), E22–E34.
Zukerberg, L.R., Patrick, G.N., Nikolic, M., Humbert, S., Wu, C.L., Lanier, L.M., Gertler, F.B., Vidal, M., Van Etten, R.A. & Tsai, L.H. (2000) Cables links Cdk5 and c-Abl and facilitates Cdk5 tyrosine phosphorylation, kinase upregulation, and neurite outgrowth. *Neuron*, **26**, 633–646.